The Preparation of Carbon-Supported Magnesium Nanoparticles using Melt Infiltration

Petra E. de Jongh,[†,*] Rudy W. P. Wagemans,[†] Tamara M. Eggenhuisen,[†] Bibi S. Dauvillier,[†] Paul B. Radstake,[†] Johannes. D. Meeldijk,[‡] John W. Geus,[‡] and Krijn P. de Jong[†,*]

Inorganic Chemistry and Catalysis, Department of Chemistry, and Electron Microscopy Utrecht, Department of Biology, Utrecht University, 3584 CA Utrecht, The Netherlands

Received August 6, 2007. Revised Manuscript Received September 17, 2007

Magnesium dihydride contains 7.7 wt % hydrogen. However, its application for hydrogen storage is impeded by its high stability and slow kinetics. Bringing the size of $Mg(H_2)$ into the nanometer range will not only enhance the reaction rates but has also been theoretically predicted to change the thermodynamic stability and destabilize the MgH_2 with respect to Mg. However, the preparation of such small particles is a major challenge. We identified a method to prepare large amounts of nanometer-sized nonoxidized magnesium crystallites. The method is based on infiltration of nanoporous carbon with molten magnesium. The size of the Mg crystallites is directly influenced by the pore size of the carbon and can be varied from 2–5 to less than 2 nm. The majority of the nanocrystallites is not oxidized after preparation. No bulk magnesium was detected in the samples with nanoparticle loadings up to 15 wt % on carbon. These 3D supported nanomaterials present interesting systems to study how nanosizing and support interaction can steer the hydrogen sorption properties of metal hydrides.

Introduction

For hydrogen storage on board vehicles, the reversible reaction of H_2 with metals at near-ambient pressures and temperatures may lead to compact systems with adequate gravimetric storage densities if the main material components are light metals.[1,2] However, the reversibility and kinetics are often limiting features. Kinetics and reversibility can be improved by doping the material with a small amount of catalyst and decreasing the crystallite size.[3–7] If the material is to absorb and desorb H_2 near 1 atm and near fuel-cell operating temperatures (roughly between 50 and 150 °C), the enthalpy of decomposition ($\equiv -\Delta H_f^0$) should be in the range of 42–55 kJ/mol of H_2.[2,8] Unfortunately, ΔH_f^0 is not in the desired range for any of the primary metal hydrides that meet gravimetric storage density criteria. Most hydrides, such as NaH, LiH, and MgH_2, are far too stable as bulk materials to enable reasonable H_2 pressures below 150 °C.[8]

Magnesium has been considered as one of the most promising materials for hydrogen storage. It is light and abundant, and magnesium dihydride contains 7.7 wt % hydrogen. However, a major impediment toward practical use is its large enthalpy of decomposition of 75 kJ/mol of H_2, which translates into an equilibrium temperature at 1 bar H_2 pressure of 288 °C. In practice, sorption temperatures of 300–400 °C are needed because of kinetic limitations, especially if no catalyst is present and passivation by surface oxidation has occurred.[5] These temperatures can be lowered by adding an extra compound that forms an alloy or compound with the magnesium, thereby decreasing the stability difference between the metal and the metal hydride.[8–10] However, for these increasingly complex systems, reversibility is often an issue because of mass-transport limitations and phase segregation. Theoretical calculations suggested that the hydrogen desorption enthalpy for pure MgH_2 also may be lower, namely, in systems with physical confinement, small crystallites, or thin layers.[11–15] Quantum-chemical calculations showed that if the crystallite size is reduced, MgH_2 destabilizes faster than Mg. As a result, for sufficiently reduced crystallite sizes (below 1 to 2 nm), the absolute value of ΔH_f^0 decreases dramatically; for 0.9 nm

* To whom correspondence should be addressed. E-mail: p.e.dejongh@uu.nl; k.p.dejong@uu.nl (P.E.d.J.).
† Department of Chemistry, Utrecht University.
‡ Department of Biology, Utrecht University.

(1) Schlapbach, L.; Züttel, A. *Nature* **2001**, *414*, 353.
(2) http://www.eere.energy.gov/hydrogenandfuelcells/storage/storage_challenges.html.
(3) Huot, H.; Liang, G.; Schulz, R. *Appl. Phys. A: Mater. Sci. Process.* **2001**, *72*, 187.
(4) Bogdanovic, B.; Schwickardi, M. *J. Alloys Compd.* **1997**, *1*, 253.
(5) Zaluski, L.; Zaluska, A.; Ström-Olsen, J. O. *Appl. Phys. A: Mater. Sci. Process.* **2001**, *72*, 157.
(6) Oelerich, W.; Klassen, T.; Bormann, R. *J. Alloys Compd.* **2001**, *315*, 237.
(7) Baldé, C. P.; Hereijgers, B. P. C.; Bitter, J. H.; de Jong, K. P. *Angew. Chem., Int. Ed.* **2006**, *45*, 3501.
(8) Alapati, S. V.; Johnson, J. K.; Sholl, D. S. *J. Phys. Chem. B* **2006**, *110*, 8769.
(9) Vajo, J. J.; Mertens, F.; Alm, C. C.; Bowman, R. C.; Fultz, B. *J. Phys. Chem. B* **2004**, *108*, 13977.
(10) Dornheim, M.; Doppiu, S.; Barkhordarian, G.; Boesenberg, U.; Klassen, T.; Gutfleisch, O.; Bormann, R. *Scr. Mater.* **2007**, *56*, 841.
(11) Liang, J. J.; Kung, W. C. *J. Phys. Chem. B* **2005**, *109*, 17837.
(12) Wagemans, R. W. P.; van Lenthe, J. H.; de Jongh, P. E.; van Dillen, A. J.; de Jong, K. P. *J. Am. Chem. Soc.* **2005**, *127*, 16675.
(13) Liang, J. J. *Appl. Phys. A: Mater. Sci. Process.* **2005**, *80*, 173.
(14) Cheung, S.; Deng, W.-Q.; van Duin, A. C. T.; Goddard, W. A. *J. Phys. Chem. A* **2005**, *109*, 851.
(15) Bérube, V.; Radtke, G.; Dresselhaus, M.; Chen, G. *Int. J. Hydrogen Res.* **2007**, *31*, 637.

10.1021/cm702205v CCC: $37.00
Published on Web 10/26/2007

MgH_2 crystallites, the enthalpy of decomposition is only 63 kJ/mol (200 °C theoretical equilibrium at 1 bar H_2 pressure) and could be reduced further for smaller particles.[12] It has also been predicted that encapsulation of $Mg(H_2)$ in a nanoscale scaffold can considerably lower the decomposition enthalpy of the hydride because of physical confinement.[13] Furthermore, it is known, for instance, for interstitial hydrides such as Pd, that stress within the material can influence the hydrogen sorption properties; recently, destabilization of the hydrides because of stress in Mg–Ti thin film systems was reported.[16] Hence, the possibility to prepare nanometer-sized particles of magnesium, interacting with or confined by a substrate or matrix, would yield interesting systems to investigate the option to lower the H_2 desorption temperature for relatively stable metal hydrides.

Nanostructuring hydrogen storage materials by ball-milling to improve kinetics and distribute dopants to the system is common practice,[17,18] but this method typically produces micrometer-sized particles consisting of crystal grains with a minimum size of 10–15 nm. Furthermore, during hydrogen cycling, the crystal grain size rapidly increases to 50–100 nm.[17] It is far from trivial to obtain smaller particles than this and stabilize nanosized particles during cycling. Wet-chemical synthesis of Mg nanoparticles in liquid ammonia has been reported, but these experiments have not been followed up.[19] With gas-phase techniques, generally only small amounts can be produced, and it is virtually impossible to prevent significant oxidation.[20,21] Very recently, Chen and co-workers reported on the gas-phase growth of unsupported magnesium nanorods that displayed enhanced hydrogen-sorption kinetics.[22,23] However, the minimum diameter of these rods was 30–50 nanometers. In this paper, we report on a method to prepare large quantities of 3D carbon-supported metallic magnesium with crystallite sizes on the order of a few nanometers.

Experimental Section

We prepared magnesium nanoparticles by infiltration of nanoporous carbon with molten magnesium. Different types of nanoporous carbons (particle size typically 20–50 μm) were explored: C_{meso} (high-surface area-graphite HSAG500-RC085 with mainly 2–3 nm pores, purity 99.9%, obtained from Timcal Ltd., Bodio, Switzerland); microporous activated carbon, 99.5% purity, without (AC_{micro} = extrudate R2030CO2) or with 10 at % oxygen ($AC_{micro\text{-}O}$ = granulate 990721) (both obtained from Norit Nederland BV The Netherlands); AC_{m+m} (activated carbon containing both micro- and mesopores and ~10 at % O, extrudate ROZ 3 A8332 obtained from Norit Nederland BV, The Netherlands); and ordered mesoporous carbon without (OMC) or with (OMC_N) a significant amount of nitrogen, prepared as described below. The $AC_{micro\text{-}O}$ was pretreated with an aqueous 25 wt % ammonia solution for 1 h under reflux, washed, and dried. Ordered mesoporous carbon was obtained following Ryoo et al. [24] SBA-15 was synthesized by dissolving 8 g of the block copolymer $ethyleneoxide_{20}$–$propyleneoxide_{70}$–$ethyleneoxide_{20}$ (P123 Pluronic) in 60 g of H_2O and 240 g of an aqueous solution of 2 M HCl, and slowly adding 17 g of tetra-ethyl-orthosilicate (TEOS, Acros Organics) at 40 °C while stirring. The solution was rested for 20 h at 40 °C, aged at 80 °C for 48 h, filtered, and dried at 120 °C. The sample was calcined at 550 °C for 6 h. The carbon replica without nitrogen was prepared by impregnation of 1 g of a dry SBA-15 in vacuum with 0.7 mL of an oxalic acid solution in furfuryl alcohol with a molar ratio of 0.0044:1. The furfuryl alcohol was polymerized by heating at 80 °C for 16 h in air. Carbonization was achieved by heating under a N_2 flow: first, for 6 h at 150 °C, and then for 30 min at 300 °C (ramp 1 °C/min), and finally, for 4 h at 850 °C (ramp 1 °C/min). The nitrogen-containing carbon replica was prepared via chemical vapor deposition using acetonitrile.[25] For 2 h, an Ar stream of 30 mL/min was bubbled through CH_3CN at 30 °C before entering a fixed bed reactor with 0.5 g of SBA-15 at 900 °C. To remove the silica, we refluxed the composites in 300 mL of aqueous 1 M KOH solution for 2 h at room temperature; they were then filtered and washed three times with 1 M KOH (aq). After this procedure was repeated, the sample was washed with water until the pH was neutral and dried overnight at 90 °C. All nanoporous carbons were ground in a mortar, dried at 400 °C, and stored under N_2 in a glovebox (Mbraun Labmaster I30, ~1 ppm H_2O, ~1 ppm O_2).

MgH_2 was obtained as a powder from Goldschmidt GmbH (~35 μm Tego Magnan). In a typical experiment, after being dried, 1 g of carbon was mixed with 500 mg of MgH_2 of similar particle size in a mortar. In an exploratory experiment, 1 g of AC_{m+m} was mixed with 500 mg of Mg and pressed for 15 min at 100 °C with 10^4 kg/cm^2 to provide intimate contact between the carbon and magnesium. Five hundred milligrams of the mixture was placed in a flash-dried alumina cup (20 × 20 × 50 mm) and transported under a nitrogen atmosphere to a tube furnace. The quartz tubes (ø 50 × 1000 mm) in the tube furnace (Thermolyne 79300) were predried at 100 °C under an Ar flow (300 mL/min). To limit the evaporation of magnesium, we placed the sample cup in a narrow alumina tube (ø 30 × 60 mm) inside the quartz tube. A cup with sacrificial MgH_2 was placed in the gas stream just before the sample as an oxygen and water scavenger. The sample was heated to 625 °C at 2.5 °C/min and kept there for 10 min before heating further to 666 °C at 1 °C/min with an Ar flow of 30 mL/min. After 10 min just above the melting point of magnesium, the samples were slowly cooled to room temperature. Around 350 °C, H_2 was introduced to replace Ar in the gas stream. After preparation, all samples were stored and handled under nitrogen.

Scanning electron micrographs (SEM) were obtained using a Philips XL30S FEG electron microscope equipped with embedded EDAX and low kilovolt backscatter detectors. Powder samples were applied dry to a conducting sticky carbon film on the sample holder. The samples were briefly exposed to air upon transfer into the electron microscopes. The TEM samples were prepared by dipping a TEM substrate (consisting of a holey carbon film on a copper grid) in the nanocomposite powder and shaking off excess material. TEM analysis was performed using an FEI Tecnai 20 FEG

(16) Borsa, D. M.; Gremaud, R.; Baldi, A.; Schreuders, H.; Rector, J. H.; Kooi, B.; Vermeulen, P.; Notten, P. H. L.; Dam, B.; Griessen, R. *Phys. Rev. B* **2007**, *75*, 205408.
(17) Zaluska, A.; Zaluski, L.; Ström-Olsen, J. O. *J. Alloys Compd.* **1999**, *288*, 217.
(18) Schimmel, H. H.; Huot, J.; Chapon, L. C.; Tichelaar, F. D.; Mulder, F. M. *J. Am. Chem. Soc.* **2005**, *127*, 14348.
(19) Imamura, H.; Usui, Y.; Takashima, M. *J. Less-Common Met.* **1991**, *175*, 171.
(20) Kimura, K.; Bandow, S. *Phys. Rev. B* **1988**, *37*, 44736.
(21) Kooi, B. J.; Palasantzas, G.; De Hosson, J. Th. M. *Appl. Phys. Lett.* **2006**, *89*, 161914.
(22) Li, W. Y.; Li, C. S.; Zhou, C. Y.; Ma, H.; Chen, J. *Angew. Chem., Int. Ed.* **2006**, *45*, 6009.
(23) Li, W. Y.; Li, C. S.; Ma, H.; Chen, J. *J. Am. Chem. Soc.* **2007**, *129*, 6710.
(24) Ryoo, R.; Joo, S. H.; Jun, S. J. *J. Phys. Chem. B* **1999**, *103*, 7743.
(25) Lu, A. H.; Kiefer, A.; Schmidt, W.; Schüth, F. *Chem. Mater.* **2004**, *16*, 100.

microscope operating at 200 kV. In bright field, virtually no contrast between carbon and magnesium was observed and hence dark-field imaging was used. To enhance detection of the nanoscale magnesium crystallites, we employed the dynamic conical dark-field mode (for more details, see the Supporting Information). X-ray diffraction patterns were collected with a Bruker-AXS D8 diffractometer equipped with a Co-Kα_{12} source (λ = 1.78897 Å). The sample holder was filled in the glovebox and closed airtight with a hemispherical X-ray transparent lid. Data were collected from 20 to 80° 2θ with a step size of 0.034° 2θ for approximately 20 min per sample. XRD was used in a semiquantitative manner to estimate the total amount of crystalline bulk Mg (for details, see the Supporting Information). N_2 physisorption isotherms were recorded with a Micromeritics TriStar 3000 apparatus at 77 K. Before measurements, the samples were dried at 250 or 300 °C under a He flow for 10 h. Single-point total pore volumes were determined at $p/p_0 = 0.995$, and pore size distributions were determined from the adsorption branch of the isotherms via the BJH method for pores between 2 and 50 nm. Pore volumes were measured before and after magnesium infiltration and after removal of magnesium. To remove the magnesium species from the composite, we mildly acid leached the sample by boiling it under reflux for 1 h in a 1 M aqueous HCl solution, followed by washing and drying.

Results and Discussion

Detection of Nanoscale Magnesium. Because of the nonpolar nature of the carbon, molten magnesium is not a priori expected to wet a carbon surface.[26] We investigated different options to improve the wetting: surface modification of the carbons with nitrogen or oxygen, and forcing metallic magnesium into the porous carbon by pressing at elevated temperature before the melt-infiltration process. However, even for some high-purity nanoporous carbons, we observed spontaneous infiltration with molten magnesium, and the formation of nanostructured magnesium upon cooling as will be discussed below. See the Supporting Information for details on the carbon morphologies.

To verify the presence of nanostructured Mg in the carbon matrix, we employed transmission electron microscopy (TEM) combined with energy-dispersive X-ray analysis (EDX). Typical results for AC_{m+m}-, C_{meso}-, and AC_{micro}-based samples containing 25–35 wt % Mg are shown in Figure 1 A–C respectively. The bright-field mode (left panels) shows the disordered structure of the carbon, but no larger crystallites. Because of the similarity in atomic weight, it is not possible to distinguish magnesium from carbon. However, in the dark-field mode (right panels), small crystallites (bright spots) could be made visible. The contrast was enhanced by using the dynamical conical dark-field mode, choosing the beam angle such that electrons diffracted because of interaction with graphitelike material were not detected (for details, see the Supporting Information). EDX confirmed that significant amounts of Mg were present inside the porous carbon particles. The average size of the nanocrystallites decreased from a few nanometers for AC_{m+m}, to ~2 nm for C_{meso} to less than 1–2 nanometers for AC_{micro}-based samples, in accordance with the decreasing pore size of the carbons.

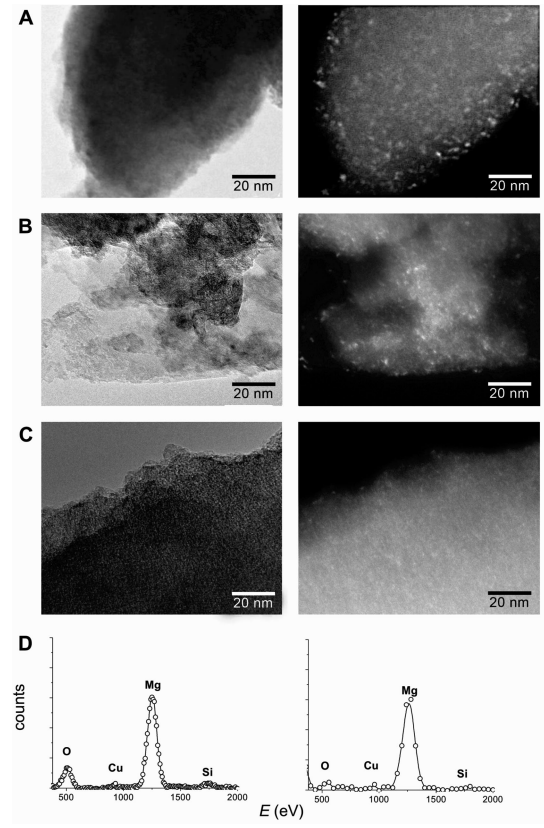

Figure 1. Bright-field (left) and dark-field (right) mode transmission electron micrographs for nanocomposites prepared from (A) 33 wt % Mg/AC_{m+m} contacted by hot pressing (B) 25 wt % MgH_2/C_{meso} and (C) 25 wt % MgH_2/AC_{micro}. Scale bar size is 20 nm. (D) EDX results for C_{meso}- (left) and AC_{micro}-based (right) samples.

Extent of Oxidation of the Nanocrystallites. Mg nanoparticles are extremely sensitive to oxidation, as was evidenced by the immediate heat production and red glow of the samples upon exposure to air after synthesis and cooling down under inert atmosphere. To reduce the oxidation sensitivity, we made it the standard procedure to replace the Ar atmosphere with hydrogen during the cooling after melt-infiltration. As the hydrogen pressure is modest, it is not expected that all magnesium is hydrided. We tentatively ascribe the protective effect to the formation of a surface hydride layer.[27] It is a challenge to determine and quantify which Mg species are present in the samples. The presence of Mg carbides is unlikely; their formation has been reported only in the presence of a carbon source that readily decomposes at the melting temperature of magnesium, such as pentane.[28,29] However, aside from Mg, MgH_2 could also be present (either as particles or as surface layer) as a result of interaction with H_2 during sample preparation. Furthermore, $Mg(OH)_2$ and/or MgO could have been formed because of oxidation. Although the total diffraction intensity from the crystallites was high enough to visualize them using dynamical conical dark-field microscopy, the rings were not intense

(26) Dujardin, E.; Ebbesen, T. W.; Hiura, H.; Tanigaki, K. *Science* **1994**, *265*, 1850.

(27) For clarity, we will simply refer to the nanoparticles as "Mg nanoparticles" in the remainder of the manuscript, although it is clear that some oxidized or hydride magnesium species might be present as well.

(28) Keiser, E. H.; McMaster, L. *J. Am. Chem. Soc.* **1910**, *32*, 388.

(29) Novák, J. *Z. Phys. Chem.* **1911**, *73*, 513.

Table 1. Overview of the Total Carbon Pore Volumes Determined from N_2 Physisorption before and after Melt Infiltration with 25 or 36 wt % MgH_2

sample	original pore volume (cm^3/g[C])	pore volume after infiltration (cm^3/g[C])	difference (cm^3/g[C])	added Mg volume (cm^3/g[C])
OMC	0.768	0.114	−0.654	0.177
OMC_N	0.543	0.217	−0.326	0.177
$AC_{micro-O}$	0.482	0.186	−0.296	0.263
AC_{M+M}	0.514	0.318	−0.196	0.263
AC_{micro}	0.450	0.324	−0.126	0.177
C_{meso}	0.649	0.567	−0.082	0.177

and sharp enough to determined which Mg species were present; only the diffraction rings due to carbon were identified. Hence, we used TEM-EDX analysis to determine the elemental composition of the Mg–C nanocomposites on selected areas of the sample where only small crystallites inside porous carbon were found. From the raw EDX data (two examples are shown in Figure 1D) it was evident that the nanoporous carbon particles contained a significant amount of Mg atoms, and that furthermore carbon, oxygen, and copper, and Si because of the TEM grid and film were present. Unfortunately, it is not possible to reliably access the C:Mg atomic ratio of the nanocomposite particles (and hence the local Mg loading), as the samples are mounted onto a carbon film for TEM analysis. To obtain quantitative atomic ratios for the other elements, we have to correct the raw data, most importantly for the absorption of low-energy radiation by the detector window. For our instrument, the correction multiplication factors for the elements C, O, and Mg are 6.3, 2.0, and 1.1. As it is essential to determine the Mg:O ratio, we verified this correction factor by analyzing MgO crystallites (produced by flame-burning of metallic magnesium wire), and our data confirmed the microscope manufacturer correction specifications.

Using the O:Mg elemental ratio, it is possible to determine whether the majority of the nanocrystalline Mg present is oxidized or not. Sometimes virtually no oxygen was detected in the selected part of the sample (see right frame of Figure 1D), but typically a small amount of oxygen was detected (see left frame of Figure 1D). Part of this oxygen usually originated from the TEM grid films, which mainly contained carbon, but often also some silicon and oxygen. Although in a typical case as presented in the left frame of Figure 1D it is not possible to unequivocally calculate the part of the Mg that is not oxidized, a best and worst case scenario can be constructed. The worst case scenario assumes that the grid films do not contribute to the oxygen signal. Then, if the O signal would be entirely due to the formation of MgO, a minimum of 50% of the magnesium would still be present in metallic (or hydride) form. If not MgO but $Mg(OH)_2$ was formed, then 70% of the Mg would still be present in nonoxidized form. In the best case scenario, all Si detected is present as SiO_2 contamination of the grid film. In this case, magnesium is not significantly oxidized. In general, we found a strong correlation between the amount of oxygen in the samples and the time that they had been stored. For samples stored for a long time and/or exposed to air, the O:Mg ratio was always close to 2, suggesting that the magnesium species is converted into $Mg(OH)_2$ upon oxidation at room temperature. However, it is clear that for freshly prepared samples, a major fraction of the nanocrystalline Mg in the samples is not oxidized shortly after preparation, not even after brief exposure to air.

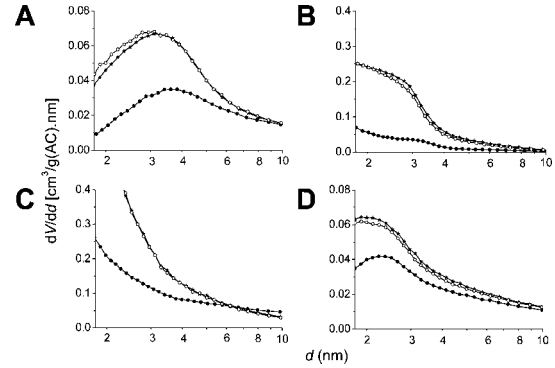

Figure 2. Carbon pore volume distributions before (—*—) and after (—•—) melt infiltration, and after removal of the Mg(O) by leaching (—○—) for nanocomposites based on (A) OMC_N, (B) OMC, (C) AC_{m+m}, and (D) C_{meso}. The nanocomposites were prepared with 36 wt % MgH_2 (C) or 25 wt % MgH_2 (A, B, D).

Interaction between the Carbon Matrix and the Molten Magnesium. Although TEM/EDX is a powerful technique to visualize Mg nanocrystallites, bulk analysis techniques are essential to obtain statistically relevant data. We used N_2 physisorption to yield information on the extent of Mg infiltration by comparing pore volumes and pore size distributions before and after contacting the C with molten Mg. An overview of the results is given in Table 1. Figure 2 shows the mesopore volume distributions, normalized to the weight of the carbon. Weight changes caused by Mg evaporation and oxidation were either negligible or compensated one other, as no significant weight change was detected upon melt infiltration. All samples showed significant pore volume losses in the range of up to 10 nm pore diameter, which is consistent with an extended interaction between the magnesium and the nanoporous carbon. Furthermore, for smaller pores, larger relative pore volume losses occurred.

Three factors can contribute to loss of pore volume: pore filling, pore blocking, or destruction of the porous nature of the carbon. To exclude the last possibility, we leached Mg from the nanocomposite with diluted hydrochloric acid. In all cases, almost all of the original pore volume was recovered. It is difficult to distinguish between pore filling and blocking, but it is illustrative to compare the loss of pore volume with the volume of the added Mg (Table 1). For the nanocomposite samples that contained a significant amount of oxygen (OMC, OMC_N, AC_{m+m}, and AC_{micro_O}), the loss of pore volume was usually greater than the volume of the added Mg. It is not surprising that these samples suffer from pore blocking, as molten Mg readily reacts with oxygen impurities to form solid MgO, which would block the pores and stop the further flow of molten Mg. For the high-purity carbons (C_{meso} and AC_{micro}), no evidence of pore blocking was found. However, this does not necessarily mean that all Mg has penetrated the pores, it is possible that part of the magnesium has blocked a large pore volume, whereas the rest is still present as bulk Mg. In general, it can be concluded that there is a sufficient interaction between molten magnesium and the carbon to bring about

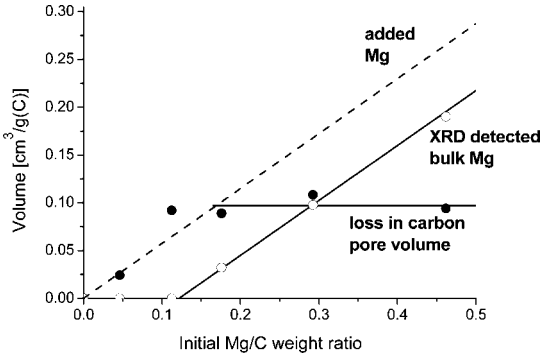

Figure 3. Comparison between the total loss of carbon pore volume as measured by N_2 physisorption (—•—), and the amount of bulk Mg detected with XRD (—○—) as a function of initial Mg/C loading for samples based on C_{meso}. The amount of Mg added is also indicated (dashed line).

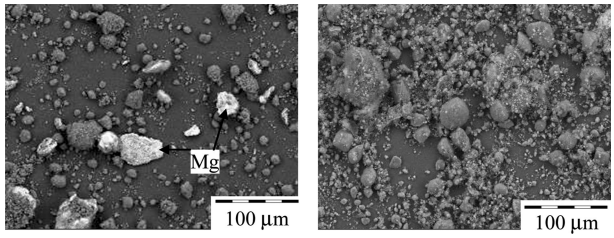

Figure 4. Backscattered electron (BSE) scanning electron micrographs of nanocomposites based on C_{meso} with different loadings, respectively, 33.3 (left frame) and 10.8 wt % MgH_2 (right frame).

capillary flow to at least partly fill pores with a diameter of 10 nm or smaller.

Quantification of the Nano versus Bulk Phase. To assess how much magnesium had penetrated into the carbon, we varied the magnesium loading for a given carbon matrix. For samples based on C_{meso}, Figure 3 compares N_2 physisorption results as a function of loading with semiquantitative XRD analysis of the bulk magnesium content (see the Supporting Information for details). Also, the volume of the added Mg is indicated. For low loadings, the loss of pore volume increases linearly with increasing magnesium loading. Furthermore, with XRD, no bulk magnesium is detected for loadings below 10–15 wt %. This combination of results suggests that at these loadings, (nearly) all of the Mg was involved in pore filling.[30] At higher loadings (for this type of carbon, >10–15 wt%), the loss of pore volume levels off and a linearly increasing amount of bulk Mg is detected with increasing loading. This suggests that above a critical loading, all extra Mg added remains as bulk material in the sample, but that below this loading, all added magnesium will be in nanocrystalline or amorphous form after preparation of the composite material.

Additional evidence comes from scanning electron microscopy. Figure 4 shows the morphology of nanocomposites based on C_{meso} after addition of 33.3 wt% (left frame) and 10.8 wt% (right frame) of MgH_2 and heat treatment. To enhance the contrast between Mg and C, we detected only backscattered electrons (BSE). In both cases, the original morphology of the carbon was retained. Additionally, for the loading of 33.3 wt%, 20–50 μm, often faceted particles are found, which by EDX could be identified as magnesium crystallites. On the other hand, for the 10.8 wt% loaded sample, no such Mg-rich particles or crystallites were detected, neither using BSE imaging nor in a higher magnification using EDX.

The "critical loading" below which no bulk Mg was detected varied with the type of carbon: for the nanocomposite based on C_{meso}, it was between 10 and 15 wt %, whereas for AC_{micro}-based composites, it was between 15 and 20 wt %. It is at this stage not yet clear what is the origin of the filling of only a specific fraction of the pores. Keeping the samples above the melting point of magnesium longer than 10 min during synthesis did not increase the pore volume loss. The fact that the amount of pore volume loss becomes independent of the amount of Mg added at high loadings suggests that the cause is not poor mixing of MgH_2 and C in the starting phase. Furthermore, experiments in which the contact was forced by pressing the physical mixture before melt infiltration, or by ball-milling, did not give a significant increase in pore volume loss. N_2 physisorption results shown in Figure 2 prove that there is a strong interaction only between the molten magnesium and pores smaller than 10 nm and that the smaller the pores, the higher the degree of pore filling. However, not all very small pores are filled. A tentative explanation is that, related to the three-dimensional character of the pores, part of the smaller pores can be accessed only via larger ones, which because of a lower effective driving force (capillary suction) are not filled with molten magnesium.

Conclusion

We prepared nanometer-sized Mg in carbon matrices. For oxygen-containing carbons, pore blocking was found, indicating, as expected, reaction between the molten magnesium and the oxygen groups on the carbon. However, several high-purity nanoporous carbons were spontaneously infiltrated by the molten magnesium. For freshly prepared samples, it was proven that the majority of the nanoscale magnesium was not oxidized. The smaller the pores, the higher the degree of pore filling; only for pores with a diameter up to 10 nm was a significant fraction of the pores filled with Mg after preparation. However, only a certain fraction of the smallest pores was filled, depending on the type of carbon. The size of the crystallites varied from 2–5 to below 2 nm by choosing carbons with different pore size distributions. As far as we know, this is the first time that results on the preparation of gram amounts of nanometer-sized nonoxidized magnesium particles are reported. Favorable hydrogen sorption properties are predicted for such small Mg nanocrystallites; we will discuss the H_2 sorption kinetics and thermodynamics in a future publication. The reported preparation route is very promising for obtaining systems in which nanosizing and substrate interaction can be used to steer the hydrogen sorption properties of light metal hydrides.

Acknowledgment. This research was funded by Utrecht University and ACTS (Project 053.61.502). P.B.R. acknowledges financial support from a Casimir Grant (018.001.001).

(30) The pore volume loss seems even somewhat higher than the volume of the added Mg. This could indicated a minor degree of pore blocking, but more likely it is due to partial oxidation of Mg to $Mg(OH)_2$, which has a larger molar volume.

We thank Ad Mens for the physisorption measurements, Marjan Versluis-Helder for the SEM measurements, and Hans Geerlings from Shell Research and Technology Centre Amsterdam for stimulating discussions. Furthermore, we are grateful to Timcal Ltd. (Bodio, Switzerland) and Norit Nederland BV (The Netherlands) for providing the high-surface-area graphite and porous carbons, respectively.

Supporting Information Available: SEM characterization of the carbon morphologies, explanation of and details on the dynamical conical dark field imaging technique for TEM, and details on the quantification of the XRD results (PDF). This material is available free of charge via the Internet at http://pubs.acs.org.

CM702205V